Requirements for Efficient Mars Launch Trajectories

LARS F. HELGOSTAM*
Lockheed Missiles and Space Company, Palo Alto, Calif.

The equations of motion are integrated numerically, utilizing a steepest-descent technique to maximize mass-into-circular-orbit. Emphasis is placed on obtaining results for a range of atmospheric models. Optimal launch accelerations, representative mass ratios, and velocity losses are presented as a function of the parking orbit altitude for a continuous-burn, constant-thrust ascent. The results show that the payload obtained is insensitive to the launch acceleration, the mass ratio is high, the dynamic pressure and the drag losses are low. Comparisons to Earth and Moon launch systems are made. A number of dual-burn ascents with coast are calculated. The results show that dual-burn gives a significantly lower mass ratio than single-burn ascent. Staging can offer considerable performance gains. It is shown that the mass in Earth parking orbit required for a Mars voyage with a continuous-thrust Mars launch system is substantially higher than that required with a dual-burn system.

Nomenclature

a = payload mass of Mars launch system divided by mass in Mars parking orbit, $a = m_p/M_m$
b = change in mass in Earth parking orbit due to different Mars launch systems normalized with respect to the mass in Earth parking orbit, Eq. (9)
D = drag
g = gravitational acceleration of Mars
I_{sp} = specific impulse
k = inert mass factor, the ratio between inert mass and propellant mass
Kap L, Kap N, Kap H = model atmospheres based on Ref. 4
M_0 = mass in Earth parking orbit
M_i = mass initially in Mars parking orbit
M_m = mass in Mars parking orbit just prior to return to Earth
m = mass
m_0 = launch mass, Mars
m_p = payload mass, Mars
n = number of stages
p = factor determined by the interplanetary mission, $M_0 = pM_i$
$\bar{q}$ = dynamic pressure
q = mass separated for launching mission from vehicle in Mars parking orbit divided by launch mass for the Mars launch system, Eq. (7)
Sch N, Sch H = model atmospheres based on Ref. 3
T = thrust
T_v = vacuum thrust
V = equivalent velocity addition for ascent, $V = g_{\text{Earth}} I_{sp} \log \mu$
V_D = velocity loss due to drag, Eq. (1)
V_G = velocity loss due to gravity, Eq. (3)
V_H = minimal velocity addition for ascent, calculated for a two-impulse Hohmann transfer
V_T = velocity loss due to thrust, Eq. (2)
α = angle of attack (inertial)
γ = flight path angle (inertial)
θ = thrust attitude angle
μ = mass ratio, launch mass divided by obtained mass-into-orbit
μ_p = payload mass ratio, launch mass divided by payload-into-orbit
τ = vacuum thrust divided by launch weight on Mars

Subscripts

1, 2 = stage 1 and 2, respectively, or case 1 and 2, respectively

Presented as Preprint 64-15 at the AIAA Aerospace Sciences Meeting, New York, January 20–22, 1964; revision received May 11, 1964.

* Senior Research Engineer.

Introduction

MANNED interplanetary voyages with the object of exploring planets in our solar system have already been subject to considerable research. The exploration of a planet most likely will involve the landing of a manned excursion module and, after an appropriate time during which the scheduled research and experiments are performed, the launch of a vehicle from the surface to a rendezvous with a mother ship in a parking orbit around the planet. Because of its proximity to us and its characteristics, Mars is the planet that currently attracts the most interest for manned landing missions.

The work described in this article is a preliminary study of the efficiency of launch trajectories from Mars and of the vehicle and flight mechanics parameters, such as number of stages and thrust level, that determine this efficiency. The most efficient combination of these parameters is determined by the planet and its atmospheric characteristics, the launch site location, the parking orbit elements, and also by the launch vehicle itself. From the flight mechanics viewpoint, the main difference today between the analytical approach to the evaluation of the launch requirements for Earth or the moon and the approach to the evaluation of the launch requirements for Mars stems from a difference in knowledge of the environments, i.e., knowledge of the atmospheres. The density of the Martian atmosphere is unknown to an order of magnitude. Therefore, the emphasis in this article is placed on finding results for different Martian atmospheric models[3, 4] and also on determining whether the launch requirements are very sensitive to the atmospheric characteristics.

The requirements are determined by calculating a number of launch trajectories that give maximum mass injected into a circular parking orbit for a given launch mass. After a vertical takeoff, the vehicle at each moment applies its thrust in the direction that will result in minimum total fuel being used for achieving the orbital conditions. Three different types of ascents are considered. In Fig. 1, a single-burn ascent is shown. A dual-burn ascent has a coast period in-

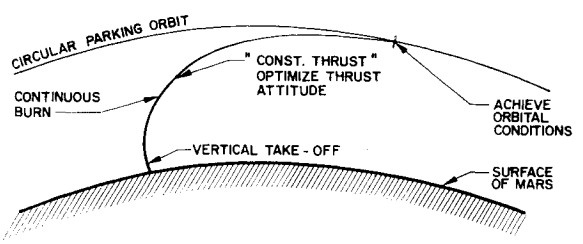

Fig. 1 Schematic ascent history.

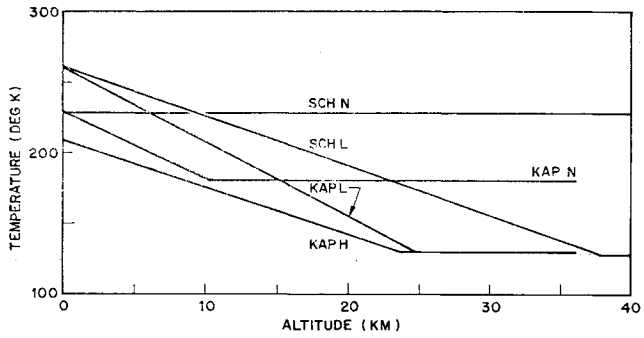

Fig. 2 Model temperature profiles for Martian atmosphere.

between the two burns, both being performed with the same stage. The two-stage ascent is similar to the dual-burn ascent, but since the second burn is performed with a second stage, inert mass can be dropped immediately after the first burn. The trajectories are calculated by numerical integration of the differential equations of the motion. The optimization of the thrust attitude is attained by a "steepest descent" iteration technique[1,2] that uses first-order partial derivatives to determine the change in thrust direction at each point along one trajectory required to obtain a specified mass improvement at the terminal point for the next trajectory.

Assumptions

The problem involves a multitude of variables. Some of them, such as the gravitational constant of Mars, are known to an appropriate degree of accuracy. Others, such as the density of the Martian atmosphere, are known to an insufficient degree of accuracy, and still others, such as the aerodynamic reference area of the launch vehicle, can be treated parametrically.

Figures 2 and 3 show temperature and density profiles for the models considered. The data for the two "Schilling" atmospheres (the nominal, Sch N, and the one with lower density, Sch L) are taken from Ref. 3. Until recently these were thought to represent a good estimate of the Martian atmosphere. The data for the three "Kaplan" atmospheres (high, Kap H; nominal, Kap N; and low, Kap L) are based on an early release of new information published by Kaplan, Münch, and Spinrad,[4] which is believed to represent the most up-to-date data for the Martian atmosphere. A good survey

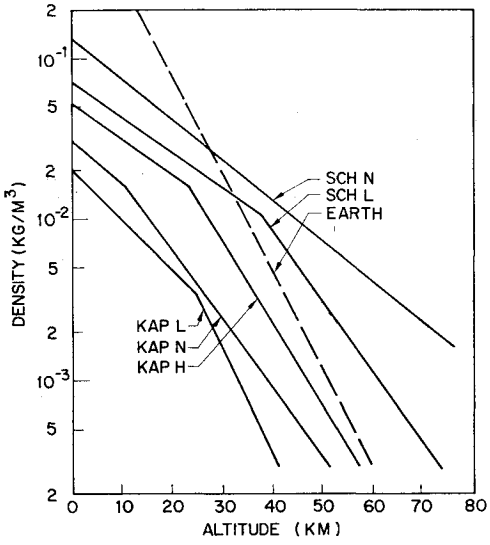

Fig. 3 Model density profiles for Martian atmosphere.

Table 1 Parameters for Mars launch study

Parameter	Constant	Variation: Parametric variation	Variation: Independent variation
For the planet:			
Atmosphere	...	Figs. 2–3	...
Gravitational constant, m^3/sec^2	$0.4296.10^{14}$	...	...
Radius, km	3385	...	...
Rotational rate, sec^{-1}	$0.7088.10^{-4}$	...	...
For the orbits:			
Altitude of parking orbit, km	...	...	100–750
Launch direction	East	...	...
Launch latitude	±20°	...	...
Launch orbit plane	Initial	...	...
For the vehicle:			
Aerodynamic reference area, m^2	6.16[a]	...	...
Drag coefficient	f of Mach number	...	...
Launch mass, kg	15,000	...	...
Lift coefficient	0	...	...
Nozzle exit area, m^2	...	$0.88\,\tau$[b]	...
Specific impulse, sec	...	315, 425	...
Thrust level	...	...	τ = 1.15–1.70[b]

[a] Corresponding to a launch mass over reference area of 500 psf.
[b] τ is the vacuum thrust divided by launch weight (on Mars).

of the theory for planetary atmospheres and a list of additional references are presented in Ref. 5.

Table 1 lists some of the parameters used for the calculations. All of the constants listed for the planet are known to a degree of accuracy sufficient for performance analysis. The parking orbit altitude is one of the independent variables. The launch trajectory is assumed to be two-dimensional. The takeoff is vertical, and the trajectory is then bent over to the East. For the vehicle, the launch mass and the aerodynamic reference area are held constant; the aerodynamic lift is neglected. The drag is represented by a zero-lift drag coefficient as a function of Mach number, similar to that of a representative Earth launch vehicle. The nozzle exit area is assumed proportional to the vacuum thrust when vehicles with different thrusts are compared. Two different values, 315 and 425 sec, are used for the specific impulse. The mass flow is assumed to be constant during the burn. The thrust-to-weight ratio τ is another independent variable.

Parking Orbit Altitude

An important parameter determined by the model atmospheres is the lowest parking orbit altitude allowed for a given vehicle and lifetime. This altitude is determined[6] by the density and the density gradient at high altitudes.

In Table 2, the altitudes for circular orbits required for a lifetime of at least 100 days are listed for satellites with M/C_DA of 3000 kg/m^2 (approximately 20 slugs/ft^2). The altitude varies little with lifetime. Note the big difference

Table 2 Parking orbit altitudes for circular orbits

Atmosphere	Altitude, km
Sch N	415
Sch L	250
Kap H	205
Kap N	225
Kap L	155

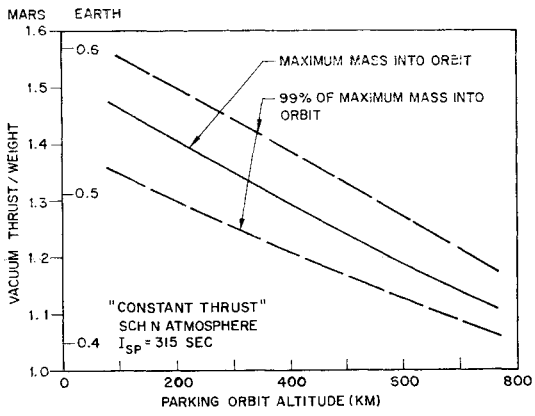

Fig. 4 Optimal launch acceleration for continuous-burn ascent.

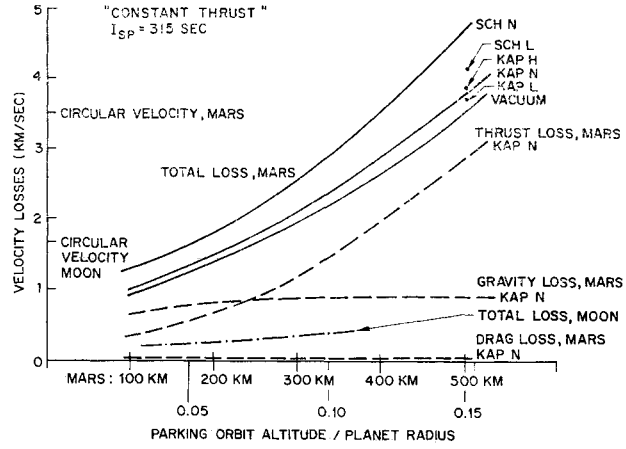

Fig. 5 Velocity losses for continuous-thrust ascent.

in required altitude for the Sch N and the Kap N atmospheres, 415 and 225 km, respectively. Even the difference between Kap N and Kap L is substantial. Due to its lower density at high altitudes, the Kap H atmosphere allows a lower parking altitude than the Kap N. For comparison, the altitude for an identical vehicle in Earth parking orbit was calculated. The result was 300 km, corresponding to nearly the same altitude-over-planet-radius as the Kap L atmosphere. For all the other atmospheres, the normalized parking orbit altitude is higher for Mars than for Earth. It should be noted that the uncertainty in the density and density gradient of the model atmospheres, and therefore in the parking altitude, is rather high. It will be shown later that the parking orbit altitude is an important parameter for the determination of the single-burn ascent efficiency.

Results

Continuous Burn

The minimum mass ratio for launch into orbit and the corresponding launch acceleration were determined by trial and error for a number of altitudes using the Sch N atmosphere. In Fig. 4, the optimal τ, the vacuum thrust divided by the initial weight on Mars of the launch vehicle, is plotted vs parking orbit altitude. The optimum is very flat. For instance, a constant τ equal to 1.30 gives a mass ratio better than 99% of the optimal for an altitude interval of 200 to 550 km. This insensitivity to launch acceleration for the continuous-burn ascent has also been observed for the moon. It can therefore be assumed to hold not only for the Sch N atmosphere but also for the other thinner atmospheres. It will be used to simplify the treatment of the problem by letting τ be a constant, 1.24, for the remainder of the continuous burn analysis.

Before examining the ascent efficiencies in detail, it is instructive to establish a feel for the various loss contributors. The total loss, $V - V_H$, is the difference in velocity addition between the calculated ascent and an ideal two-impulse Hohmann transfer. To get a measure of the components of loss, we define the following:

Drag Loss

$$V_D = \int \frac{D}{m}\, dt \qquad (1)$$

Thrust Loss

$$V_T = \int \frac{T_v - T\cos\alpha}{m}\, dt \qquad (2)$$

Gravity Loss

$$V_G = V - V_H - V_D - V_T \approx \int g \sin\gamma\, dt \qquad (3)$$

The last integral in Eq. (3) extends only over the burn time (no coast included).

The total losses calculated are shown for the two nominal atmospheres and for vacuum in Fig. 5. One point for each of the other atmospheres is shown. The Kap N loss is broken down into its components. It is evident that the Kap N drag loss is negligible. The Sch N drag loss is estimated to be the main part of the difference between the Sch N and Kap N total loss curves, increasing from 0.3 km/sec for 100 km to 0.9 km/sec for 500 km. These are still small losses compared to the others.

The dynamic pressure histories are shown in Fig. 6 for ascents to 500 km. Similar curves were obtained for lower altitudes. Note the very low values, more than an order of magnitude smaller than for Earth (here represented by data for a Saturn C-5 two-stage vehicle). This is caused by the lower density at sea level of the Martian atmospheres, and also to the lower acceleration of the launch vehicle, which implies that the higher velocities (and the dynamic pressures) are reached later (at higher altitudes) than for Earth. Thus, the maximum dynamic pressure is lower, since the density decreases rapidly with increasing altitude. The low dynamic pressure explains why the drag loss is small and indicates that the results obtained are insensitive to the assumed drag coefficient, aerodynamic reference area, and launch mass.

The second contributor is the thrust loss, which increases rapidly with increasing altitude. At higher altitudes, it constitutes the main part of the total loss. The bulk of the thrust loss is due to large angles of attack late in the boost trajectory. Figure 7 explains this. Here some representative thrust attitude histories are shown for ascents to 100 and 500 km. Because of the low thrust-to-weight ratio, the thrust remains nearly vertical for a relatively long period of time.

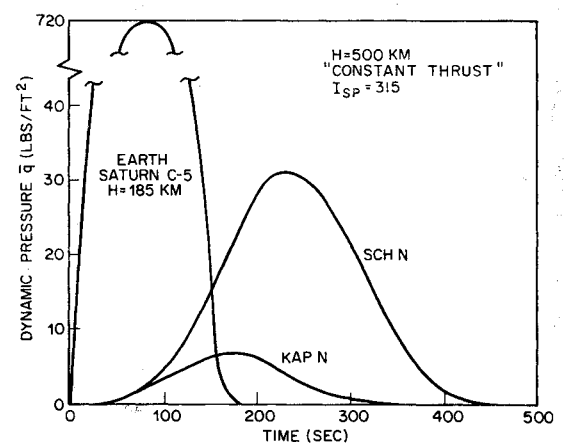

Fig. 6 Dynamic pressure history.

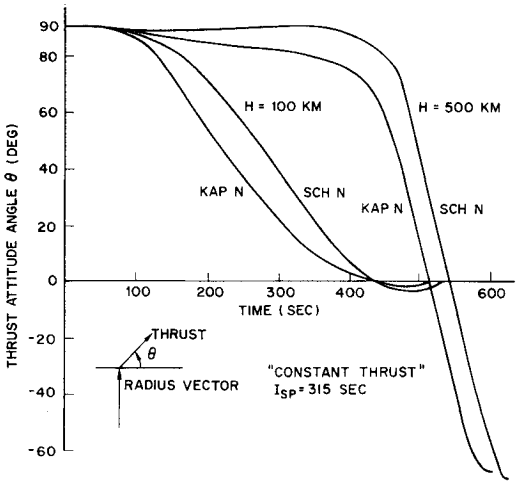

Fig. 7 Thrust attitude history.

The obtained mass-into-orbit is rather insensitive to the details of the thrust attitude program, as long as the integral of the curve does not change. The angle of attack is small for the first part of the trajectory but large at the end during the "pushover" maneuver to zero path angle. The part of the thrust loss due to the atmospheric pressure is small, as can be seen by comparing the total losses for the Martian atmosphere and vacuum in Fig. 5.

The final loss contributor is that normally associated with gravity. For this study it has been defined simply as the remaining losses [Eq. (3)]. Although the gravity loss is nearly constant, this is somewhat misleading. The thrust loss due to angle of attack is really partially attributable to gravitational effects.

In summary, the losses for continuous-burn ascents are composed almost entirely of thrust and gravity losses, with the thrust loss predominating at the higher altitudes. Representative losses for ascents from the moon are also included in Fig. 5. There is a big difference in losses between the moon and Mars, even for vacuum and small altitudes. This difference is explained by the lower gravity and the lower circular velocity for the moon.

The over-all performance efficiency expressed by the minimum mass ratio (two-impulse Hohmann transfer) divided by the obtained mass ratio is shown in Fig. 8. The efficiency is comparable to that for a Saturn C-5 two-stage Earth launch system but is much lower than that for the moon. The difference between the results for the two nominal atmospheres is notable, but the Kap N curve differs little from the vacuum curve. The increase of the specific impulse from 315 to 425 sec gives considerable improvement in efficiency for higher altitudes. This can be explained in the following way. The thrust-over-launch weight is the same

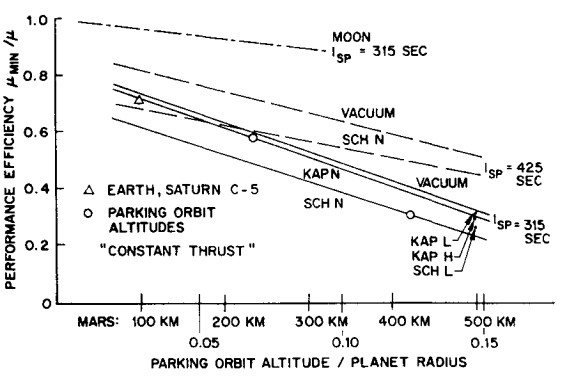

Fig. 8 Performance efficiency for continuous-thrust ascent to circular orbit.

Table 3 Continuous-burn ascent mass ratios, I_{sp} = 315 sec

Atmosphere	Parking altitude, km	Efficiency	Mass ratio	Payload mass ratio
Sch N	415	0.30	10.5	210
Sch L	250	0.50	6.2	13
Kap H	205	0.59	5.2	9.0
Kap N	225	0.57	5.4	9.6
Kap L	155	0.64	4.7	7.6

for the two cases; therefore, the higher specific impulse gives a lower acceleration in later portions of the trajectory. This alleviates the pushover maneuver and decreases the thrust losses without increasing the gravity losses, because the main part of these is built up during the early part of the trajectory where the difference between the trajectories is small.

Assuming equal parking orbit lifetimes, the mass ratio required for each of the atmospheres can be derived from Table 2 and Fig. 8. The results are listed in Table 3. Payload mass ratios μ_p are based on an inert mass to propellant mass ratio of 0.10. The high Sch N payload mass ratio indicates that a single-burn ascent should not be considered for constant thrust systems. Even for the thinnest atmosphere, the efficiency is low. The difference in payload mass ratio for the Kap atmospheres stems from the difference in parking orbit altitude. The main effect of the atmosphere is evidently to set the requirement for the parking orbit altitude.

Having obtained the results with certain parameters fixed, we can generalize them somewhat by predicting their sensitivity to changes in those parameters. Since the drag loss is a small part of the total loss, the mass ratio must be insensitive to changes in the aerodynamic reference area and the drag coefficient. A change in launch mass, holding the thrust-over-weight ratio constant, will only change the drag loss, [Eq. (1)]. A change in nozzle exit area will change the thrust loss only slightly since the main part of this is due to the angle of attack. Since the rotational velocity of Mars at the equator is 0.24 km/sec, or less than 7% of the ideal velocity addition for an ascent, the ascent efficiencies are insensitive to changes in the launch site or the launch direction. Thus the results presented for constant-thrust, single-burn ascents can be considered general in the sense that moderate variations in the parameters discussed previously will not introduce significant changes.

Dual Burn

The low efficiencies computed for high altitudes for the single-burn ascent were found to be partly the result of high angles of attack that have to be applied at the end of the

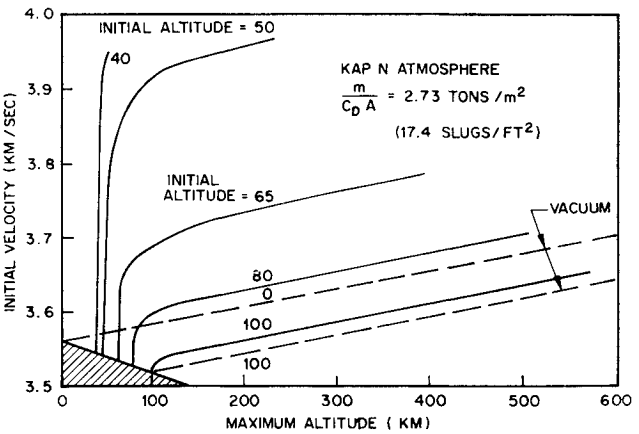

Fig. 9 Velocity requirements for coasting ascent.

Table 4 Dual-burn ascent mass ratios, I_{sp} = 315 sec

Atmosphere	First burnout altitude, km	Final altitude, km	Mass ratio	Efficiency	Coast time, min
Kap N	50	225	4.22	0.73	36
	73 (opt)	225	4.16	0.74	41
	100	225	4.28	0.72	45
	73	400	4.26	0.74	53
Sch N	140	415	5.7	0.53	55

trajectory. This, together with the facts that the Kap atmospheres are very thin and that the efficiency for ascents to lower altitudes is relatively high, indicates that a substantially higher efficiency can be obtained by introducing a coast in the ascent. The following strategy was chosen for the dual-burn ascent: Perform a first burn to an altitude "just above" the atmosphere and to a velocity higher than circular for that altitude, then coast up to the desired altitude, and employ a small second burn to achieve orbital conditions.

A number of coast trajectories were calculated for the Kap N atmosphere. Figure 9 shows the velocity required to coast, starting with a zero flight path angle, to a given maximal altitude as a function of the altitude where the coast starts. It can be seen from the figure that for 60 km and higher, little more than circular speed is required to reach high altitudes. Thus, for these altitudes, the first burn will be very similar to the single ascents discussed previously, and the results obtained regarding velocity losses and optimal thrust for these can be directly used here. The total mass ratio can be calculated using the results presented in Figs. 8 and 9 and treating the last burn analytically. The velocity addition for this burn is small, less than 100 m/sec. Its losses therefore are negligible for a wide range of thrust levels.

The results of the calculations are shown in Fig. 10 and Table 4. The corresponding result for a dual burn in the Sch N atmosphere is also estimated. The efficiency is much higher than for the single-burn ascent, except for low altitudes. By a small increase in the velocity at the first burnout altitude, a considerable increase in final altitude will be obtained, just as for a Hohmann-type transfer. Therefore, the efficiency of the dual-burn ascent is nearly independent of the final altitude. The sensitivity to changes in the first burnout altitude is also small, as is shown in Fig. 10. The dynamic pressure for circular speed at the optimal altitude, 73 km, is about 5 psf.

Effect of Staging

The results for the dual-burn ascent can be used to evaluate the effect of staging on the performance. A simple analytical approach is taken which also allows a comparison between different planets. To see the effect of staging we have to look at the payload mass ratio. Assuming a two-stage vehicle, giving the two mass ratios μ_1 and μ_2 for the two stages, respectively, the obtained payload mass m_p becomes

$$m_p = m_0 \frac{[1 - k_1(\mu_1 - 1)][1 - k_2(\mu_2 - 1)]}{\mu_1 \mu_2} \quad (4)$$

where m_0 is the initial mass and k_1 and k_2 are inert mass factors for stage 1 and 2, respectively. For the staged system, m_p has a maximum for a certain relation between μ_1 and μ_2. If k_1 and k_2 are equal and independent of μ_1 and μ_2, this relation is $\mu_1 = \mu_2$. Assuming that this optimal relation holds for the two-stage vehicle and that the total mass ratio is $\mu = \mu_1\mu_2$, Eq. (4) can be written in the general form

$$m_p = m_0[f(\mu)/\mu] \quad (5)$$

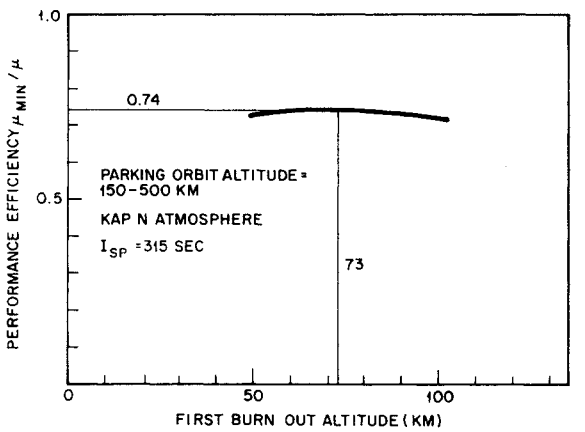

Fig. 10 Performance efficiency for dual-burn ascent to circular orbit.

$$f(\mu) = (1 - k(\mu^{1/n} - 1)^n \quad (6)$$

where n is the number of stages. The function $f(\mu)$ is plotted in Fig. 11. For a comparison between the two-stage and the dual-burn systems, they are assumed to have the same μ.

From Fig. 11, an improvement of approximately 15% in payload can then be estimated for a two-stage vehicle as compared to a one-stage dual-burn vehicle for Mars. However, this performance advantage will have to be weighed against the increase in complexity. For the moon, only a minor improvement will be obtained. For Earth, staging is necessary, and it can be seen from Eq. (6) that a three-stage vehicle can be advantageous.

Implications of Results

The results presented in this article can be used to estimate the difference in mass in Earth parking orbit prior to a Mars voyage, because of different Mars launch system efficiencies. An equation can be derived from the mass M_0 in Earth parking orbit as a function of the payload mass ratio μ_p for the Mars launch system. Assume the following for a given mission: 1) the mass in Earth parking orbit is proportional to the mass M_i initially in Mars parking orbit, $M_0 = pM_i$, and 2) the mass separated from M_i for the landing mission is proportional with the factor q to the launch mass m_0. Then two expressions for the mass in the parking orbit, assumed constant during the exploration period, can be formed:

$$M_i - qm_0 = M_m - m_p \quad (7)$$

where M_m is the mass in Mars parking orbit just prior to the return trip. The second equation is obtained by using Eq. (5), $m_0 = \mu_p m_p$, in combination with $M_0 = pM_i$ to get

$$M_0 = pM_m[1 + a(q\mu_p - 1)] \quad (8)$$

where $a = m_p/M_m$. Equation (8) relates the mass in Earth

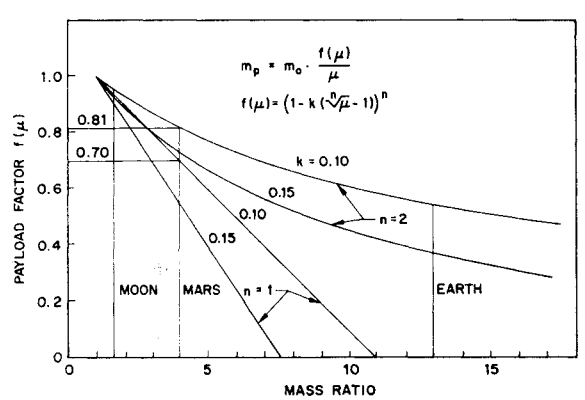

Fig. 11 Effect of staging on ascent performance.

Table 5 Sensitivity of Earth park orbit mass to Mars launch system changes

Mass launch system	Mars payload mass ratio, μ_p		Earth mass differ., b%			
	Sch N	Kap N	Sch N		Kap N	
Single burn	210	9.6	460	420	10.5	8.0
Dual burn	11	6.2	7.5	0	2.4	0
Staging	7.7	5.2	0		0	

parking orbit to the payload mass ratio μ_p of the Mars launch system.

Let the subscripts 1 and 2 designate two different Mars launch systems, respectively, for the same Earth-Mars-Earth voyage, and let us compare the corresponding masses in Earth parking orbit. From the expression

$$b = (M_{02} - M_{01})/M_{01} \tag{9}$$

since M_m can be assumed to be the same for the two cases, we get

$$b \approx aq(\mu_{p2} - \mu_{p1})/(1 + aq\mu_{p1}) \tag{10}$$

Equation (10) shows that the relative change in Earth parking orbit mass between the two missions is proportional to the difference in payload mass ratio for the Mars launch system. It helps us resolve the basic tradeoff between reliability and cost (i.e., mass in Earth parking orbit). The following example illustrates a possible Mars voyage: $a = 0.020$, and $q = 1.40$. Table 5 is based on these values. The results show how the efficiency in the Mars launch systems carries over to the required mass in Earth parking orbit. The savings by using dual-burn instead of single-burn systems is large. The saving in using two stages instead of one dual-burn can also be significant, particularly for the denser Mars atmospheres.

Conclusions

The dual-burn ascent with a coast above the atmosphere has a much higher efficiency than the continuous-burn ascent, regardless of the atmosphere model. A two-stage vehicle offers a significant improvement in performance compared to a one-stage, dual-burn vehicle. The efficiency of the dual-burn and two-stage ascent is insensitive to the final parking orbit altitude but will vary somewhat with the initial injection altitude. The efficiency of the continuous-burn ascent, on the other hand, is sensitive to the required parking orbit altitude, which, in turn, is determined by the atmosphere.

The velocity losses due to the atmosphere are small (100 to 200 m/sec) for the Kap atmospheres. They are more significant (400 to 1000 m/sec) for the Sch N atmosphere. The drag loss is negligible for thin atmospheres, and the maximum dynamic pressure during the ascent from Mars is more than an order of magnitude smaller than that for Earth.

References

[1] Bryson, A. E. and Denham, W. F., "A steepest-ascent method for solving optimum programming problems," J. Appl. Mech. **29**, 247–257 (1962).

[2] Rosenbaum, R., "Convergence technique for the steepest-descent method of trajectory optimization," AIAA J. **1**, 1703–1705 (1963).

[3] Schilling, G. F., "Limiting model atmospheres of Mars," Rand Rept. R-402-JPL (August 1962).

[4] Kaplan, L., Münch, G., and Spinrad, H., "An analysis of the spectrum of Mars," Astrophys. J. **139**, 1–15 (1964).

[5] Rasool, S. J., "Structure of planetary atmospheres," AIAA J. **1**, 6–19 (1963).

[6] Jensen, J., Townsend, G., Kraft, J., and Kork, J., *Design Guide to Orbital Flight* (McGraw-Hill Book Co., Inc., New York, 1962), Chap. V.